STRUCTURAL AND AC ELECTRICAL PROPERTIES OF MOLYBDENUM TRIOXIDE ADDED LI-CU-MG-ZN FERRITES SYNTHESIZED VIA SOLID STATE REACTION TECHNIQUE

Md Asafur Rahman[1], Ujjwal Nag[2], Samir Ullah[2], Rahima Nasrin[1,*]

[1] Department of Physics, University of Barishal, Barishal – 8200, Bangladesh.
[2] Department of Physics, Bangladesh University of Engineering and Technology (BUET), Dhaka 1000, Bangladesh.

Abstract

In this study, the effect of Molybdenum Trioxide (MoO_3) adding on the structural and AC electrical properties of Li-Cu-Mg-Zn ferrites (LCMZF) has been investigated. The samples were synthesized through solid-state reaction technique and sintered at 1100°C. X-ray diffraction analysis confirmed that all the samples are single-phase cubic spinel assembly. The dielectric properties of the samples exhibited diffusive activities ensuing the Maxwell-Wagner nature of polarization. The dielectric constant of MoO_3 added LCMZF is larger than that of pristine LCMZF, that may be ascribed to the densification of the sintered samples resulting in enhancement of polarization. Cole-Cole plot indicates that the conduction mechanism occurs through the both grain and grain boundary contributions. The conductivity of 0.5 wt% MoO_3 added LCMZF samples are larger in compared to the other samples.

Key words: Ac Electrical Properties, Molybdenum trioxide, Li-Cu-Mg-Zn Ferrites, Solid state reaction technique.

Introduction

The arranged magnetic materials have a fascinating region of study because of their conceivable applications in a variability of broad zones extending from information technology to biotechnology (Patil et al., 1991 and Jie. et al., 2010). Spinel ferrites clay is broadly used in microwave devices to regulator transmission route, frequency, generosity and phase of microwave signals. The electrical transmission and dielectric behavior of ferrites significantly depend on the preparation circumstances likely sintering temperature, chemical structure, extent and nature of additives. Deflation of AC electrical properties with frequency in polycrystalline ferrites is sharply contingent on the polarization method (Ahmed et al., 2004 and Khan. et al., 2013). Precise dielectric and magnetic properties dimension at the operative frequency and temperature limits are required to support the manufacturing of the ferrites (Hakim et al., 2000). The utmost popular amalgamations are Ni-Zn (Huq et al., 2008), Ni-Cu-Zn (Ajmal and Maqsood, 2013), Mg-Zn (Bahadur et al., 2005) and Mg-Cu-Zn ferrites (Snoek, 1984). These ferrites supply a group of magnetic materials suitable for radio and TV sets as carrier telephony. Furthermore, polycrystalline lithium-zinc (Li-Zn) ferrites are favorable materials that have been broadly used in microelectronic productions as well as telecommunication technology due to their momentous properties such as elevated magnetic permeability, good dielectric constant, comprehensive band absorption frequency area, low electrical conductivity, elevated mechanical strength, and rapid dielectric loss (Abbas et al., 1995 and Akhter. et al., 2011). A large number of investigation has been conducted on the field of ferrite to understand the different properties of the sample for their suitable application and different preparation technique. (Hasan et al., 2023) prepared $Cu_{0.2}Zn_{0.2}Ni_{0.6-}$

*Corresponding author: Rahima Nasrin Mukta (nasrin77@gmail.com)

$_xMg_xFe_2O_4$ nanoferrites by co-precipitation method. The X-ray diffraction (XRD) pattern confirmed the cubic spinel (CS) structure and the replacement of Ni^{2+} with Mg^{2+} ions of synthesized ferrites. The average crystallite size was decreased whereas the lattice constant increased with the accumulation of Mg^{2+} concentration. The specific surface area value ranges from 52.51 to 67.83 m^2/g for the synthesized nanoferrites, signifying that soft ferrites might be used for supercapacitors. The fourier transform infrared spectral (FTIR) revealed the dispersal of ions on the tetrahedral site sideways through force constant. The observed DC resistivity confirms the semiconducting nature of soft ferrites. The value of direct and indirect band gap ranged from 3.40 to 3.68 eV & 0.84–1.03 eV, respectively. (Gabal et al., 2021) investigated the structural and Ac-electrical properties of nanocrystalline metal ferrites (MFe_2O_4, M = Co, Ni, Cu, Mg, and Zn) prepared through autocombustion process. The crystallization of the entire ferrites are cubic spinel's structure as observed by XRD analysis. The FTIR analysis exposed the distinctive vibration bands of ferrites. The transmission electron microscope (TEM) pictures displayed clustered particles with cubic morphology for all samples. The determined magnetization values differ with the nature of the metal ion, and $CoFe_2O_4$ exhibited the highest one. The temperature and frequency-dependent Ac-conductivity designated semiconducting behaviors. With the increase in temperature, the conduction mechanism is altered. The attained low dielectric constant values suggest high-frequency applications namely microwave devices of the samples. (Mazen et al., 2021) studied the electrical features of the Mn/Co/Cu-substituted Ni–Zn ferrites prepared via citrate technique. The frequency-dependent dielectric parameters have been analyzed using Maxwell and Wagner's model. Two semicircles consistent to the grain and grain boundary were detected from the Cole-Cole plot. The replacement of Ni ions by Mn/Co/Cu ions designates a key advancement in the Ac-dielectric behaviors of Ni − Zn ferrite suggesting the suitability for high-frequency devices. (Ingale et al., 2023) evaluated the structural, and electromagnetic behaviors of Co^{2+} replaced NiCuZn Ferrites(NCZF). XRD study established the vastly crystal-like single-phase CS assembly. With the increase of Co addition into the ferrite system the loss of porous gel structure is observed by field emission scanning electron microscope (FESEM) investigation. The energy dispersive x-ray spectroscopic study revealed the existence of Ni, Cu, Zn, Co, and O in NCZF samples. With the addition of Cu ions, the electrical conductivity of ferrites is increased. In contrast, with the increase in frequency, the dielectric constant of ferrites decreases. (Firozuddin et.al., 2021) investigated the frequency-dependent dielectric behaviors of V_2O_5 -added NCZF. They observed a reverse correlation between the dielectric constant as well as AC electrical conductivity in the samples. The electrical resistivity of V_2O_5 -doped NCZF are observed to be larger than that of pure NCZF.

From the review, it is seen that the electrical and magnetic behaviors of ferrites depend on numerous dimensions like the formulation method, reaction distribution, sintering temperature, type and quantity of fundamental replacement. A chemical addition may play an important role in developing the mass transport mechanism because of the existence of the liquefied phase at the sintering procedure. Earlier, different types of supplement oxides namely V_2O_5, SiO_2, MoO_3, and Bi_2O_3 were conduct as an additive to impact microstructure, electrical and magnetic properties. However, to the best of our knowledge there is no report available on the complex permeability, dielectric features of MoO_3-substituted Li-Cu-Mg-Zn compounded ferrites (LCMZF). There is a lack of analysis of the influence of MoO_3 implantation on the complex magnetic permeability, dielectric property and impedance spectroscopy of LCMZF. In this regard, a detailed study has been scheduled to explore the frequency-dependent dielectric constant and Ac electrical conductivity of MoO_3 substituted LCMZF (MOSLCMZF) together with the micro-structural features. In this research we represent the structural and Ac electrical behaviors of MOSLCMZF prepared by solid state reaction (SSR) technique. The structural and Ac electrical properties were studied by the powder X-ray diffraction and Ac impedance analyzer respectively.

Materials and Methods

The composite LCMZF was synthesized via conventional SSR technique. Purified powders of MgO, ZnO, CuO, $LiCO_3$ and Fe_2O_3 were balanced and admixed with distilled water. The mixed material was ball-milled at a rotating speed of 250 rpm for 4 h. After that they were dehydrated up and heat treated at 800°C for 3 h. Different wt% of MoO_3 powders were correspondingly mixed with it at the lower sintering temperature. After the next ball-milling for 6 h, the mixes were dried up for crystalize with polyvinyl acetate (PVA) mixed as a binder. Then the constituent parts were hard-pressed into rings and disks at 8 MPa pressure. As a final point, the samples were heat treated at 1100°C in a heating system. Flow chart of sample preparation procedure is represented in Fig.1

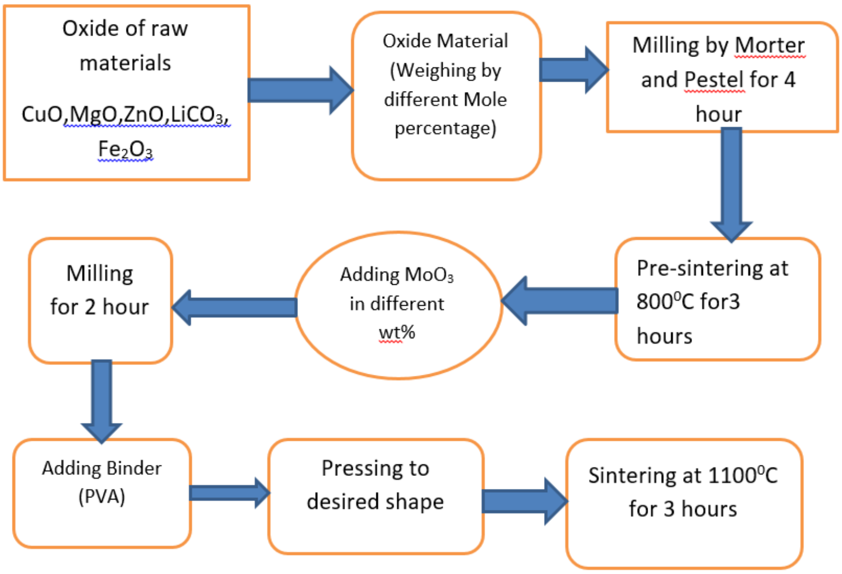

Fig. 1 Flow chart of sample preparation procedure

The structural properties of LCMZF and MOSLCMZF were characterized by the powder XRD technique at ambient temperature using Philips X-ray diffraction functioning with Cu-Kα radiation. The diffraction patterns were noted down in the 2θ range of 10° to 70°. The Ac dielectric properties were evaluated in the frequency range of 100Hz - 1MHz using an Ac impedance analyzer, Wayne Kerr, 6500B, UK.

Results and Discussion

Structural analysis

Fig.2 displayed the XRD pattern of prepared MOSLCMZF with different MoO_3 contents. The fundamental reflection planes (111), (220), (311), (222), (440), (422), (333) and (440) confirmed the single-phase cubic spinel structure of the samples. The lattice spacing '*d*' using the equation from Bragg's law (Seo et al., 1999)

$$2d_{hkl}\text{Sin}\theta = n\lambda \quad (1)$$

$$\text{i.e. } d_{hkl} = \frac{\lambda}{2\text{Sin}\theta} \quad (2)$$

where, λ is the X-ray wavelength, θ is the diffraction angle and n is an integer.

The lattice constant was computed by using the equation (Zhang et al., 2004):

$$a = d_{hkl} \times \sqrt{h^2 + k^2 + l^2} \quad (3)$$

where, h, k, l are the crystal planes.

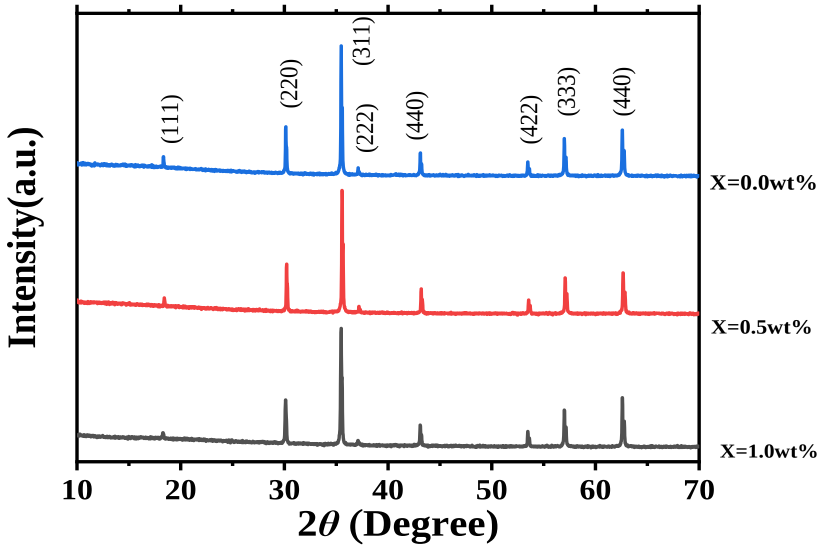

Fig. 2: XRD pattern of MOSLCMZF with different MoO_3 contents sintered at 1100°C

Bulk density

The bulk density (ρ_B) was computed using the equation:

$$\rho_B = \frac{Mass\ of\ sample}{Volume\ of\ Sample} = \frac{m}{V} = \frac{m}{\pi r^2 h} \quad (4)$$

where, *m* is the mass of sample, *r* is the radius of the sample and *h* is the thickness of the tablet.

.

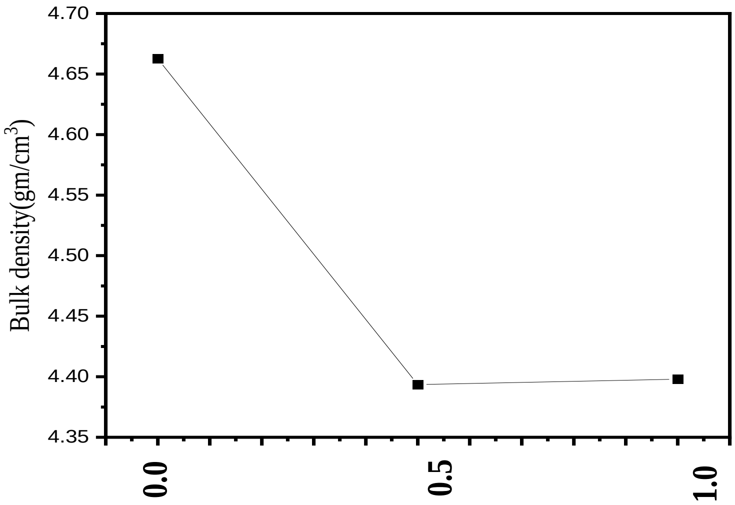

Fig. 3: Variation of bulk density of MOSLCMZF with different MoO_3 contents.

.The variation of ρ_B of MOSLCMZF with different MoO_3 contents is demonstrated in Fig.3. In general, the ρ_B of material displays a linear correlation with sintering temperature. However, it tend to decrease when deformation of material take places (> sintering temperature). The ρ_B of MOSLCMZF decreases with the increase of MoO_3 contents due to the grain of particles growth. The X-ray density, ρ_x was also computed from the following equation (Gu et al., 2009):

$$\rho_x = \frac{MZ}{Na^3} \tag{5}$$

Where, Z is the , N is the and M is the molecular weight of the form. All the calculated lattice constants and bulk density of the prepared samples are presented in Table 1.

Table 1: Lattice parameter and bulk density for MOSLCMZF with different MoO_3 contents

MoO_3 Contents (wt%)	Lattice constant a (nm)	Bulk density ρ_B (g/cm^3)
0.0	0.838	4.66
0.5	0.837	4.39
1.0	0.836	4.39

Dielectric properties

Dielectric constant

The dielectric constant (ε′) is a conclusive factor concerning microelectronic applications of dielectric materials. The value of ε′ was computed using the following equation (Dawoud et al., 2006):

$$\varepsilon' = \frac{C_p d}{\varepsilon_o A} \tag{6}$$

where C_p *is the* capacitance of a parallel plate capacitor, d represents the separation between the plates, ε_o represents the permittivity of the free space and A is the area of each plate. The Variation of ε' with frequency (f) at different MoO_3 contents is presented in Fig. 4. At this point the dielectric constant was calculated over comprehensive frequency at ambient temperature (27ºc). It is revealed that the ε' decreases continuously with increasing f for all the samples. The lessening of ε' with rising f is a regular performance of ferrites. The dielectric dispersion is speedy at lower f area and stays nearly impartial at higher f. Ferrites hold a well-conducting grain disparate by imperfectly conducting grain boundaries. It is also be observed that the ε' of 0.5 wt% MOSLCMZF is higher than that of pure LCMZF.

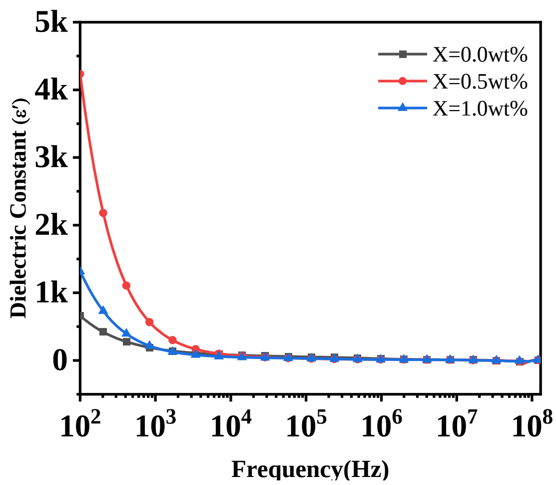

Fig. 4: Variation of ε' with f of MOSLCMZF at different MoO_3 contents

Loss factor

The quality factor is a vital parameter in lenient ferromagnetic materials because the extent of energy consumed in processes other than magnetization can avoid the application of AC from a given material. The ratio of ε'' and ε' is a measure of the inefficiency of the magnetic system, equal to tanδ, which represents the loss factor in the material. The loss factor, tanδ can be calculated using the formula (Akter et al., 2011):

$$\tan\delta = \varepsilon''/\varepsilon' \tag{7}$$

The variation of tanδ, with the frequency of all samples are demonstrated in Fig.5 The tanδ value is maximum when the electron frequency is almost the same as the functional frequency which is due to the effect of ferromagnetic character. The lower Tanδ value is observed at a higher frequency region owing to grain transfer action. In contrast, the higher value of tanδ in the lower-frequency region is due to the grain boundary effect. The electrical losses of MoO_3 may give way for the LCMZF observed at higher frequencies to be implemented in high-frequency devices.

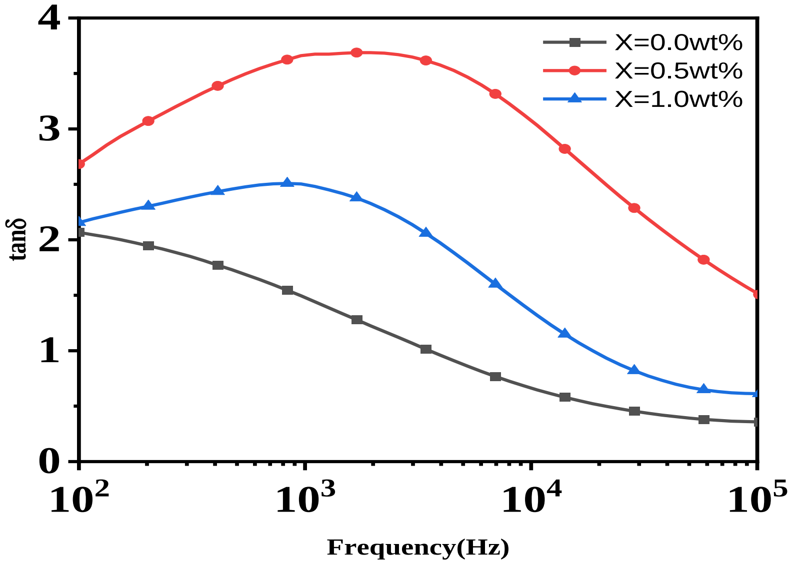

Fig. 5: Alteration of tanδ with *f* of MOSLCMZF at different MoO_3 contents

Electrical transport properties

Impedance spectroscopy

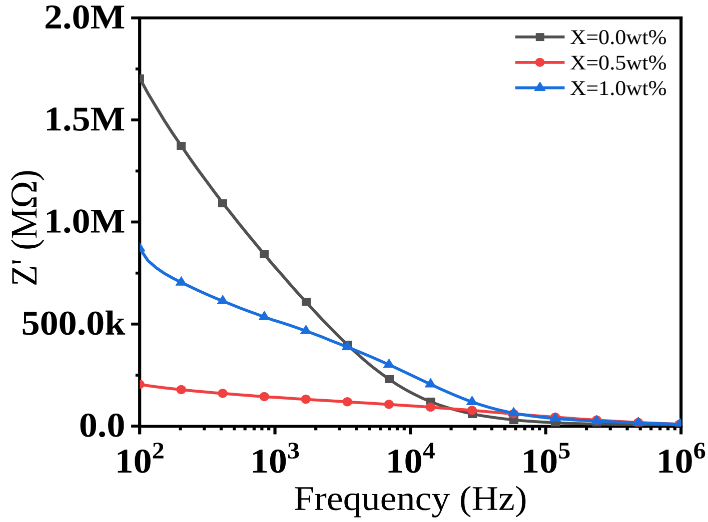

Fig. 6: Alteration of Z′ with f of MOSLCMZF at different MoO_3 contents

The dimension of impedance is an important issue in getting information about the electrical transportation mechanism of MOSLCMZF. The complex impedance provides the info near the resistive (Z′) and reactive (Z") constituents of the MOSLCMZF. Fig. 6 displays the disparity of Z′ with the applied frequency of several MOSLCMZF samples.

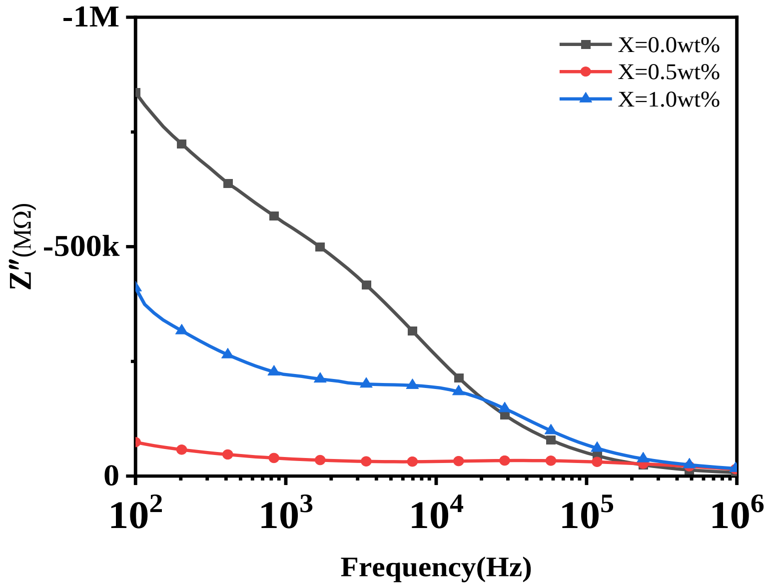

Fig. 7: Variation of Z″ with frequency of MOSLCMZF at different MoO_3 contents

It is noticed that Z′ slowly declines with the rise of frequency, suggesting that A electrical conductivity surges with f for all MOSLCMZF samples. The Disparity of Z″ with the frequency of several MOSLCMZF samples is displayed in Fig. 7. It exhibits dispersion because of the existence of space charge lessening character in that material. At higher frequencies, both Z′ and Z″ are found to be frequency-independent in nature, which also correlated to the drop of space-charged polarization on the grain boundaries.

Cole-Cole plot

Owing to understanding the effect of grain and grain boundary on the Ac-electrical behaviors of various MOSLCMZF at different MoO_3 contents, Cole-Cole plots have been observed. According to the equivalent circuit, impedance can be written as (William, 2003):

$$Z^* = R_g - \frac{1}{j\omega_g C_g} + R_{gb} - \frac{1}{\omega_{gb}\ C_{gb}} \qquad (8)$$

where, R_g, R_{gb} and C_g and C_{gb} are the grain and grain boundary (GAGB) resistances and capacitances respectively, while w_g and w_{gb} are the frequencies for the GAGB respectively. The Cole-Cole plot of various MOSLCMZF samples are depicted in Fig 8. The Cole-Cole diagram shows the contribution of GAGB to the total resistance of the structure. The radius of the semicircle for 0.5% MOSLCMZF samples are lowered compared to other samples. It indicates that the conductivity of 0.5% MOSLCMZF samples are larger in compared to the other samples.

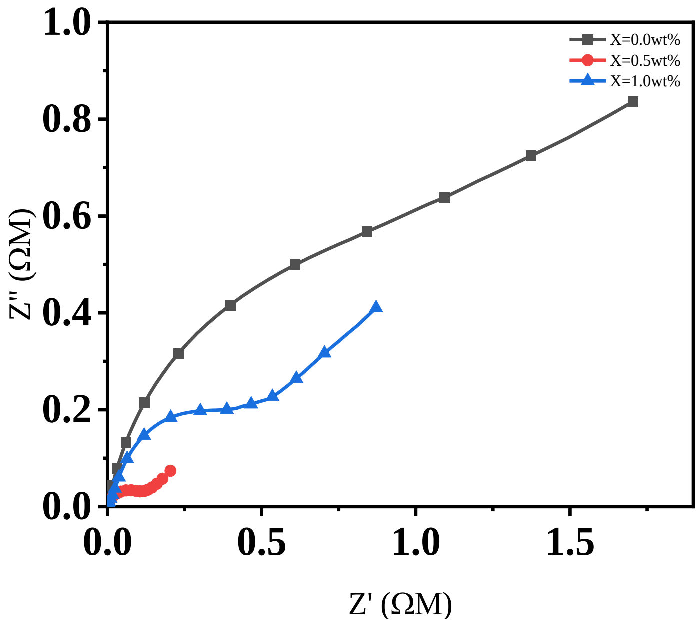

Fig.8 : Cole-Cole plot of various MOSLCMZF at different MoO_3 contents

Conclusion

In this study, MoO3-added LCMZF have been prepared via solid-state reaction technique and structural and Ac electrical properties of these samples have been investigated. XRD analysis displayed that the addition of a small amount of MoO_3 had no visible impact on spinel phase LCMZF. The alteration of ε' with *f* value has exhibited the standard dielectric dispersion. Impedance spectroscopy analysis confirmed that the samples have a grain effect on electrical properties. The Cole-Cole plots demonstrated the resistance of the samples declined with MoO_3 content which indicated a non-Debye type relaxation. The conductivity of 0.5% MOSLCMZF samples is larger in comparison to other samples. The lower value of tanδ for MOSLCMZF indicates its possible application in high-frequency devices.

Acknowledgement

Research facilities provided by BUET are greatly appreciated. The authors would like to acknowledge the XRD analysis facilities at the Materials Science division, BAEC, Dhaka. One of the authors (Md Asafur Rahman) thanks the authorities of Barishal University, Bangladesh (Barishal-8200) for permitting to carry out this research activity.

References

Patil R. S., Kakatkar S. V., Patil S. A., Maskar P. K. and Sawant S. R. 1991. Dielectric Behaviour of $Li_{0.5}Zn_xTi_x Fe_{2.5-2x}O_4$ Ferrites; Physica. Status Solidi a 126 (2): 185-193.

Jie S., Lixi W., Naicen X., Qitu Z. 2010. Introduction to Ferrite; Journal of Rare Earths. 28: 445-451.

Ahmed T. T., Rahman I. Z. and Tofial S. A. M. 2004. Effect of Copper in distribution on the magnetization of nanoscaled Ni-Zn ferrites; Journal of Magnetism and Magnetic Materials, 272: 2250 – 2252.

Khan Z. H., Mahbubur Rahman M., Sikder S. S., M. A. Hakim and D. K. Saha. 2013. Complex Permeability of Fe deficient Ni-Cu-Zn ferrite; Journal of Alloys and Compounds. 548:208 - 215.

Hakim M. A., Manjurul Haque M., Huq M., Manjura Hoque Sk. and Norbblad P. 2000. Reentrant Spin Glass Behavior of Diluted Mg-Zn Ferrite; CP 1003, Magnetic Materials International Conference on Magnetic Materials, AIP. P295.

Huq M.M and Huq M. and Hakim M. A. 2008, Thermal hysteresis of Permeability and Transport properties of Mn Substituted Mg-Cu-Zn ferrites. Journal of Physics D: Applied Physics, 41:1 – 10.

Ajmal M and Maqsood A. 2008. Structural, electrical and magnetic properties of $Cu_{1-x} Zn_xFe_2O_4$; Journal of Alloys and Compounds. 460:54 – 59.

Bahadur D., Giri J. Nayak B. B., Sriharsha T., Prasad N. K. 2005. Processing, Properties and Some Novel Applications of Magnetic Nanoparticles. Journal of Pramana Physics. 65:663-669.

Snoek J. L.1984. New development of Ferromagnetic Materials; Elsevier Publ. Co. N.Y.

Abbas T., Islam M. U. and Choudhury M. A. 1995. Study of sintering behavior and electrical properties of Cu-Zn-Fe-O system; Modern Physics Letters. 9:1419 – 1426.

Akhter S., Paul D., Hakim, M. A., Saha, D., Al-Mamun A. and Perveen A. 2011: Synthesis, structural and physical properties of $Cu_{1-x} Zn_xFe_2O_4$ ferrites; Material Science and Applications. 2(11):1675 – 1681.

Hasan, M. S., Ali, S. S., Rizwan, M., Khan, M. I., Ullah, H. N., & Irfan, M. I. 2023. Structural, optical, electrical and magnetic properties of CuO. ZnO. 2NiO. 6-xMgxFe$_2$ O$_4$ (x= 0.00, 0.15, 0.30, 0.45, 0.60) soft ferrites. Journal of Alloys and Compounds. 956:170392-6.

Gabal, M. A., Katowah, D. F., Hussein, M. A., Al-Juaid, A. A., Awad, A., Abdel-Daiem, A. M., ... & Asiri, A. M. 2021. Structural and magneto electrical properties of MFe$_2$ O$_4$ (M= Co, Ni, Cu, Mg, and Zn) ferrospinels synthesized via an egg-white bio template. *ACS omega*. *6*(34): 22180-22187.

Mazen, S. A., Nawara, A. S., & Abu-Elsaad, N. I. 2021. Investigation of dielectric behavior in $NiO_{7-x}ZnO.3M_xFe_2O_4$ (M= Mn/Co/Cu) ferrites by impedance spectroscopy. *Ceramics International*. *47*(7):9856-9865.

Ingale, B., Nadargi, D., Nadargi, J., Suryawanshi, R., Shaikh, H., Alam, M. A. & Suryavanshi, S. S. 2023. Evaluation of Structural, Magnetic, and Electromagnetic Properties of Co^{2+} -Substituted NiCuZn Ferrites. ACS omega. *8*(33:30508-30518.

Firozuddin, M.F, Ullah, M.S., Hoque, S.M., Khan, F.A., Momin, A.A., Islam, S.R., Salehin, F. and Hakim, M.A.. 2021. Electrical transport properties of V_2O_5-added Ni–Co–Zn ferrites. J. Advanced Dielectrics. 11(06):2150025-6.

Seo, S.H. and Oh, J.H.. 1999. Effect of MoO/sub 3/addition on sintering behaviors and magnetic properties of NiCuZn ferrite for multilayer chip inductor. IEEE transactions on magnetics. 35(5):3412-3414.

Su, H., Zhang, H., Tang, X. and Xiang, X.. 2004. High-permeability and high-Curie temperature NiCuZn ferrite. Journal of magnetism and magnetic materials, 283(2):157-163.

Gu, M. and Liu, G. 2009. Effects of MoO_3 and TiO_2 additions on the magnetic properties of manganese–zinc power ferrites. Journal of alloys and compounds. 475(1):356-360.

Dawoud H. and Shaat S. 2006. Magnetic properties of Zn substituted Cu ferrites; An-
Najah Univ. J. Res. (N. Sc.).20: 87 – 100.

Akter S, Hakim M.A and Al-Mamun Md. 2011. Synthesis, structural and physical properties of $Cu_{1-x}Zn_xFe_xO_4$Ferrites; Material Science and Applications. 2:1675 - 1681.

William D. C. 2003: The University of Utah: Materials Science and Engineering 6th Ed., Wiley.